



Brine palaeocurrent analysis based on oriented selenite crystals in the Nida Gypsum deposits (Badenian, southern Poland)

Maciej B BEL

B bel M. (2002) — Brine palaeocurrent analysis based on oriented selenite crystals in the Nida Gypsum deposits (Badenian, southern Poland) *Geol. Quart.*, 46 (4): 435–448. Warszawa.



Unique sedimentary structures indicating the direction of brine currents are present in the Middle Miocene (Badenian) evaporite basin in Carpathian Foredeep. They occur within widespread gypsum deposits cropping out along the northern margin of the Foredeep, in Ukraine, Poland and the Czech Republic. The primary bottom-grown selenite crystals show apices turned horizontally in the same or similar directions, and are interpreted as the direction of inflowing calcium sulphate oversaturated brine. The upstream directed crystals are used to reconstruct brine palaeocurrents in outcrops of the Nida Gypsum deposits in NW margin of the Foredeep evaporite basin in Poland. Palaeocurrent analysis is based on simplified measurements which consisted in the determination of azimuth intervals enclosing groups of conformably oriented crystals. Measurements revealed that the brine flowed into the study area mainly from north and east, and outflowed farther towards the SW. This palaeoflow is roughly parallel to the basin margin contour and is a part of the longshore counterclockwise brine circulation well documented in other areas of the basin. Local deviations from the uniform flow directions suggest presence of shoals and islands forming obstacles for the brine streamlines on the Nida area.

Maciej B bel, Institute of Geology, University of Warsaw, Al. wirki i Wigury 93, PL-02-089 Warszawa, Poland; e.mail: babel@geo.uw.edu.pl (received: March 15, 2002; accepted: July 24, 2002).

Key words: palaeocurrent analysis, brine, gypsum crystals, sedimentology, evaporites.

INTRODUCTION

The Middle Miocene (Badenian) gypsum deposits of Carpathian Foredeep basin exposed in western Ukraine, Poland and Czech Republic reveal perfectly preserved primary sedimentary structures (Kwiatkowski, 1972; Kasprzyk, 1993a, b; Peryt, 1996, 2001; Petrichenko *et al.*, 1997). One of the unique structures of these deposits are the conformably orientated bottom-grown selenite crystals which apices are inclined and turned horizontally in one direction. This peculiar feature was also noticed in the other Miocene evaporite basins, such as the Sorbas Basin in Spain (Dronkert, 1977, 1978, 1985), the Caltanissetta Basin in Sicily, and the Vena del Gesso Basin in northern Italy (B bel and Lugli, unpublished), and was interpreted by several authors (Dronkert, 1977, 1978, 1985; Pawlikowski, 1982, remarks on p. 36; B bel, 1986, 1996) as a result of growth of selenite crystals towards the brine current supplying ions necessary for the crystal building. The conformable orientation of selenite crystals is a regionally observed feature which allows reconstruction of the general pattern of brine flow in the Badenian evaporite basin in Carpathian Foredeep (B bel *et al.*, 1999).

Numerous measurements made in Ukraine, and in some selected outcrops in Poland and the Czech Republic, indicated that the brine generally flowed along the coast of the basin in counterclockwise direction similar to observations in many recent closed and semi-closed basins in northern hemisphere where such a counterclockwise water circulation is attributed to an effect of Coriolis force.

This paper presents brine palaeocurrent analysis based on oriented selenite crystals in the Nida Gypsum deposits, in a small (15 x 30 km) part of evaporite basin in northern Carpathian Foredeep in Poland. Because of the many exposures with oriented selenites the Nida area offers the best insight into a pattern of palaeocurrents in the Polish part of the basin. Some random palaeocurrent data were already published from that area (B bel, 1996, fig. 16; B bel *et al.*, 1999, fig. 1). Oriented selenite crystals were measured by Niemczyk (1997, ryc. 3).

The purpose the present paper is twofold. First, to introduce methodology of palaeocurrent reconstruction based on simplified field measurements of selenite crystals orientation. Secondly, to reconstruct pattern of brine palaeoflows on the Nida area and discuss some sedimentological and palaeogeographic aspects of this reconstruction.

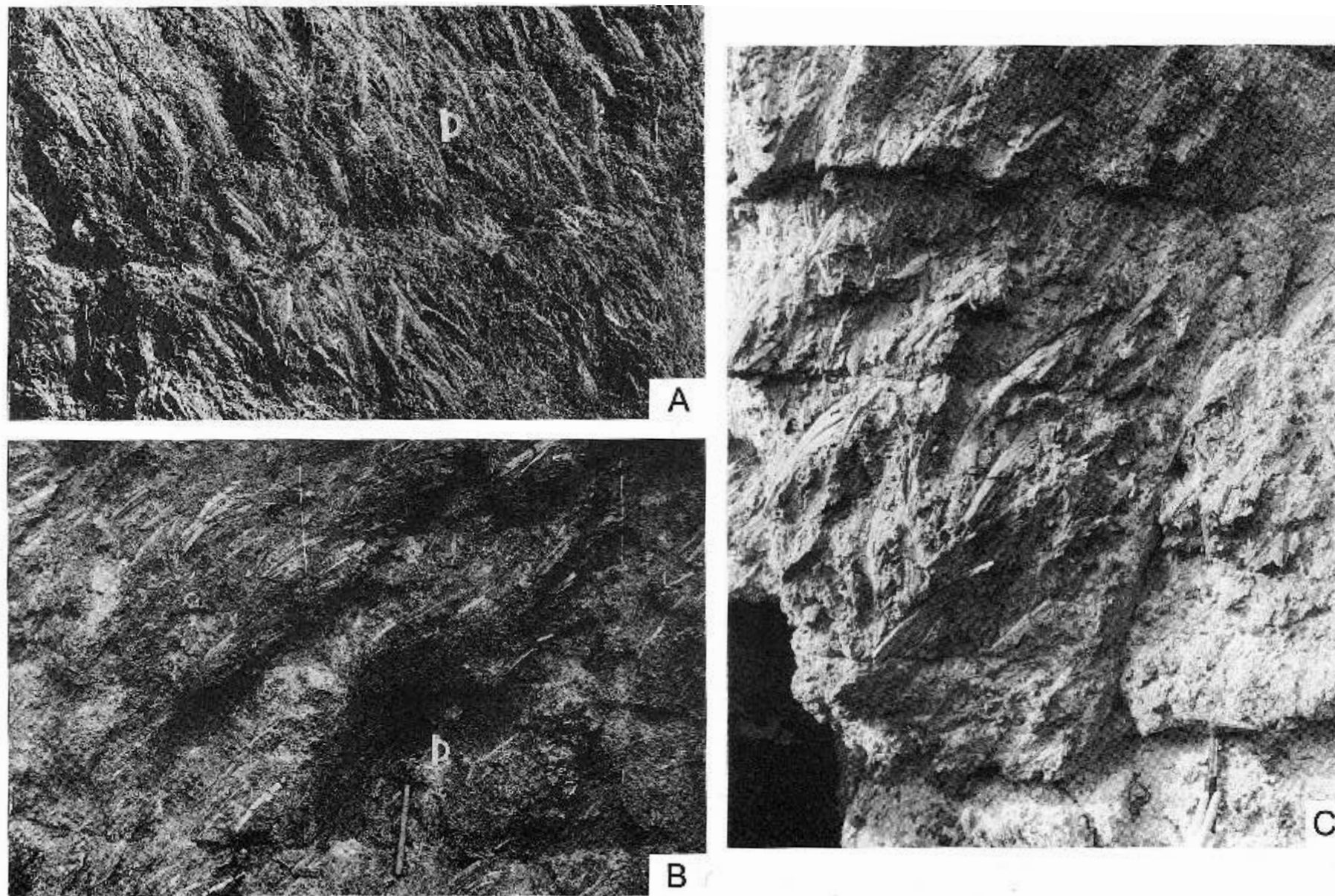


Fig. 1. Conformably oriented sabre gypsum crystals in layer g

A — Gartatowice, locality 13, protractor used as a scale is 10 cm long; B — Siesławice, locality 37; C — Skorocice, locality 55

GEOLOGY OF THE NIDA GYPSUM DEPOSITS

The Nida Gypsum deposits crop out in the Nida River valley at vicinity of Busko, Wi lica and Pi czów. The gypsum exposures mark the west-north erosional extent of Badenian evaporites which to the south and east occur in the subsurface (Kwiatkowski, 1972, 1974; Kubica, 1992; Kasprzyk, 1993a, b). The studied deposits locally reach over 50 m in thickness. The lower member (16–19 m thick) is better preserved and exposed part of the sequence is mainly composed of bottom-grown selenites, the upper member is composed of microcrystalline gypsum. The selenites are represented by several sedimentary facies of which the most widespread and important for the present study are: the sabre gypsum and the grass-like gypsum (B el, 1999a, b, with references). The Nida Gypsum sequence comprises seven lithosomes, lettered from **A** to **G** by Kubica (1992), which are divided into about 15 characteristic layers lettered from **a** to **m** (Wala 1961, 1963, 1980; B el, 1996, 1999b). The distribution of these layers in the studied outcrops is shown in Wala (1961, 1963), Kasprzyk (1994, figs. 3 and 4) and B el (1996, table I; 1999b, figs. 2 and 3). The strata are laterally continuous and show similar thickness in nearly the whole northern Carpathian Foredeep (Kasprzyk, 1993a, b, 1995; Petrichenko *et al.*, 1997; Peryt, 1996, 2001). The great lateral continuity is attributed to layer by layer deposition on a very flat substrate.

These selenite layers (lettered, Appendix 1) were recognized in the field mainly by characteristic lithologic features such as arrangement, sizes and morphology of crystals, content and structure of fine-grained gypsum “matrix”, as well as other sedimentary structures like dissolution surfaces or microbialites. Because the layers are laterally continuous their constant position within the gypsum sequence helped in their recognition in some pure exposures. Layers **g** and **i** are separated by thin characteristic “marker” bed **h**. Layers **b** and **d** are very similar in lithology and were recognizable by contacts with layers **c** and **e** containing spectacular gypsum microbialites (Kwiatkowski, 1970, 1972; Kasprzyk, 1993a; B el, 1999).

STRUCTURES INDICATING BRINE FLOW

ORIENTED GYPSUM CRYSTALS IN THE SABRE FACIES

The structures indicating the brine flow direction are very common within one of the most widespread Badenian selenite facies — the sabre gypsum. The name of the sabre facies derives from its makeup, being narrow (less than 5 cm), long (up to several tens of cm) and curved gypsum crystals resembling sabres (Fig. 1A, B) and described as the sabre crystals (B el, 1999a, fig. 5B). The crystals are primary and were grown directly on the bottom of evaporite basin under permanent cover of calcium sulphate oversaturated brine. They grew upward and simultaneously curved horizontally forming ordered rows or clusters. Shorter several cm long rod-like crystals and {100} twins grew among the sabre crystals being attached to their surfaces (Fig. 1C). The best recent analog of this sabre facies and

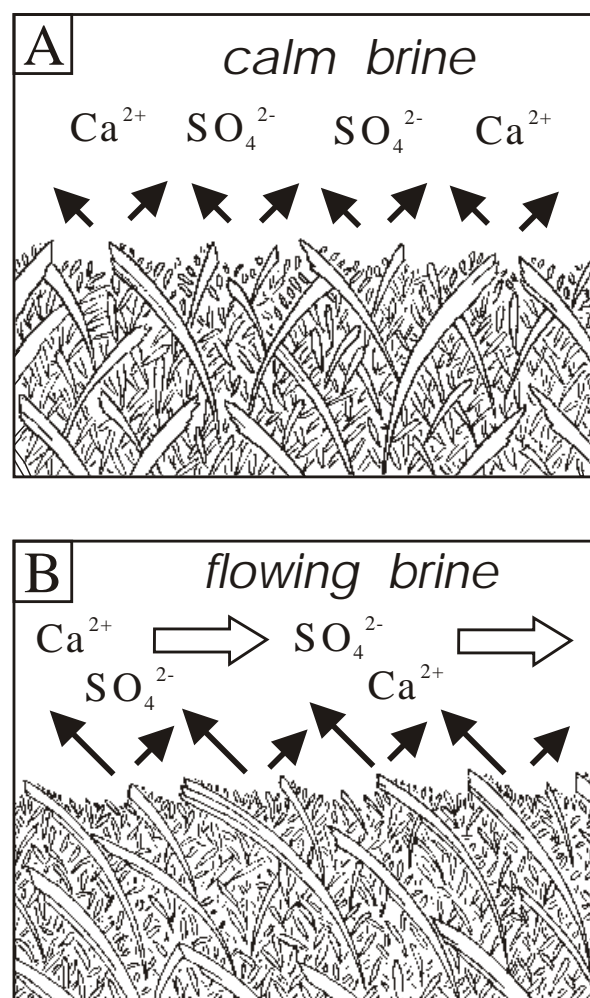


Fig. 2. Scheme showing competitive growth of sabre crystals

A — in a calm brine; **B** — in a flowing brine; length of solid black arrows corresponds to the rate of crystal growth

of the sabre crystals is described from the marine salinas of Spain (Ortí Cabo *et al.*, 1984).

Depositional environment of the discussed facies was unanimously interpreted by Kasprzyk (1993a, b), B el (1996, 1999a) and Peryt (1996, 2001) who claimed that the selenites crystallized in density stratified brine having a maximum depth of several metres which commonly was moving in the same direction. Many environmental factors influenced the peculiar morphology, curved habit, and arrangement of bottom-grown gypsum crystals (B el, 1986, 1996, 1999a). The most important control for the crystal fabric development was that sabre crystals grew exclusively by advance of the apical {120} (or related) faces while the growth of the side faces close to {111} was completely inhibited, probably by an adsorbed layer of specific organic compounds (Cody and Cody, 1991; Cody and Cody, 1991; B el, 2000). The selenite crystallization was also influenced by movement of brine. A consistent brine flow accelerated the growth rate of upstream oriented crystal faces and produced structures indicating the palaeoflow directions in the following manner (B el, 1996).

Similarly as crystals growing on the common substrate (as in mineral druses) all the sedimentary selenite crystals com-

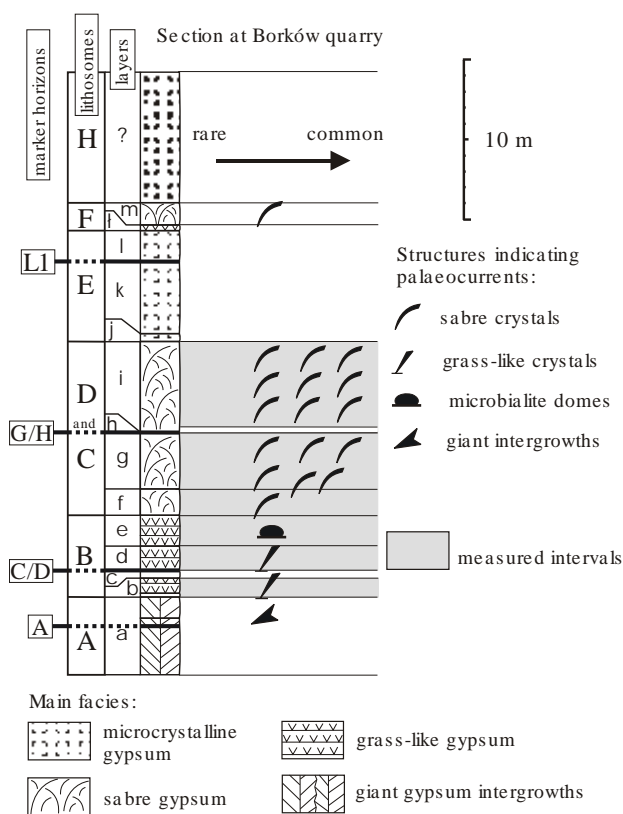


Fig. 3. Distribution of measured palaeocurrent indicators in the Nida Gypsum sequence in the representative Borków section; layers after Wala (1963, 1980, supplemented and modified), lithosomes after Kubica (1992); marker horizons *cf.* B bel (1996, 1999b); main facies after B bel (1999a, b)

peted for free space during the growth on the bottom of evaporite basin. The largest crystals, i.e. the sabre crystals, are the “winners” or “survivors” in this competitive growth process known also as geometric selection. They grew protruding over the average bottom level and surpassing the smaller crystals growing in depressions between them. The smaller crystals did not have a chance for full development due to the lack of free space occupied by adjacent large crystals growing upward faster. It is interpreted that when growing in still or slowly moving brine the longest sabre crystals spread their apices upward and radial in every horizontal direction in equal number because the crystal growth rate was the same in all directions (Fig. 2A). However, when calcium sulphate oversaturated brine was flowing permanently over the crystallizing selenites the sabre crystals with apices directed towards the inflowing brine grew faster than the other ones (as it was observed in some experiments; Newhouse, 1941; Prieto *et al.*, 1996; Hilgers and Urai, 2002). This led to preferential selective development of upstream directed crystals (Fig. 2B), while the other differently oriented crystals were surpassed and eliminated from the competitive growth (like in the computer model of the growing crystal aggregates by Rodriguez-Navarro and Garcia-Ruiz, 2000). The apices of ancient sabre crystals showing the same or similar horizontal orientation are thus excellent indicators of brine flow paths.

The discussed structures are the most purely developed within layer **f** (Fig. 3). Commonly they are lacking in the lower part of this layer where the sabre crystals are absent or very rare

and short (less than 15 cm). The longer (commonly 25–30 cm) sabre crystals appear in transitional area between layer **f** and **g**, and are more frequent going up of the section. Upstream orientation of sabre crystals is also more and more apparent up-section. The longest (30–40 cm, maximum up to 95 cm) conformably oriented sabre crystals are recorded in layer **i**. The crystals do not show a pronounced orientation within layer **m2** which is purely exposed and thin.

ORIENTED CRYSTALS IN OTHER GYPSUM FACIES

Upstream orientated selenites are rarely observed in the grass-like facies (Fig. 3). They appear among the 5–20 cm long straight bottom-grown crystals which create aggregates resembling grasses. Unlike the sabre crystals the grass-like aggregates commonly represent one generation of crystals. The crystals show rod-like habit and morphology different from the sabre crystals (B bel, 1999a, fig. 5A). The conformable orientation of the grass-like crystals is related to the same processes as described above. The horizontally oriented selenites locally occur also in the giant intergrowths facies (in the non-palisade subfacies; see Fig. 3, B bel, 1999a, pl. III, fig. 1; 1999b, fig. 2). However, because of the competitive growth structures are not clearly visible, the palaeocurrent significance of this orientation is controversial.

SOME OTHER STRUCTURES INDICATING PALAEOCURRENTS

Elongated microbial gypsum domes occurring within the grass-like facies (Figs. 3 and 4) are interpreted as parallel to the currents (*cf.* Kwiatkowski, 1970, 1972) by analogy to modern stromatolite domes on tidal flats.

METHOD OF MEASUREMENTS

The upstream oriented sabre (and other) crystals are not ideally parallel. Their apices form a dispersed “fan” within some interval of azimuth directions. The intervals, depending on place, show a span from less than 45° to over 180°. The precise documentation of dominating crystal orientation (or orientations) requires statistic measurements of many individual sabre crystals (B bel *et al.*, 1999; Roman, 1999). In case of very dispersed directions of apices the measurements should be very frequent (practically over 100). Such measurements are time-consuming and because of that a precise brine palaeocurrent reconstruction requires long-termed field studies.

In this paper another simplified method of measurements is introduced. In each outcrop, or group of nearby outcrops, only two azimuths were identified and measured, those ones limiting the interval enclosing all the azimuths indicated by the single apices of sabre crystals (or the most of them). The measured pair of limited azimuths, i.e. the left limited azimuth and the right limited azimuth, is described in this text as the azimuth interval and the angle between them (enclosing the sabre crystals) as the azimuth span. The azimuth intervals drawn on the map are described as the azimuth fans.

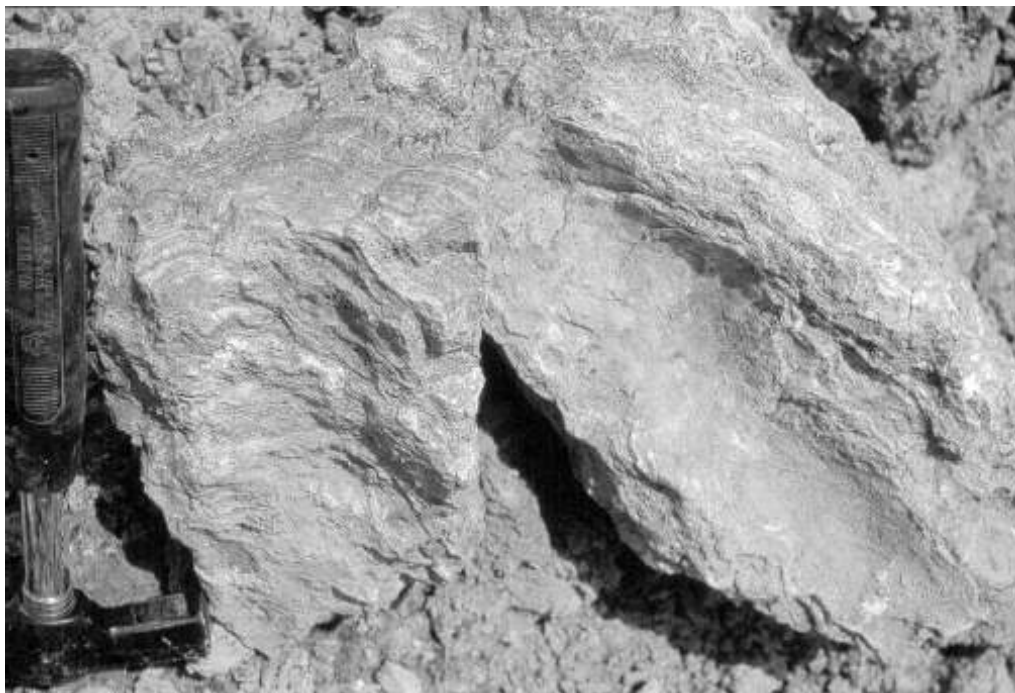


Fig. 4. Elongated gypsum microbialite domes, layer e, Borków, locality 17

Field determination of the azimuth intervals is relatively univocal for well oriented sabre crystals characterized by narrow azimuth spans less than 90° . Such azimuth intervals practically enclose all the sabre crystals seen in outcrop. However, in places where the apices are dispersed in nearly every horizontal direction and azimuth intervals are broad (azimuth span over 120°), identification and measuring of the limited azimuths is difficult. They are purely visible and were determined much more subjectively. The measurements were approximated within 5° . The author always tended to enlarge measured azimuth spans to make the possible palaeocurrent directions to be surely placed within azimuth intervals. Although only a pair of measurements was enough for one outcrop, usually several pairs of measurements were made in different walls of the same outcrop, or in adjacent outcrops, and from them two azimuths enclosing all the measurements were selected (Appendix 1).

The conformable orientation of sabre crystals is generally the same throughout several metres thick intervals of the section (some deviations are possible to detect only by statistic measurements of individual sabre crystals). For this reasons commonly only one measured azimuth interval was enough for one outcrop.

INTERPRETATION OF MEASUREMENTS

PALAEOCURRENTS IN SINGLE OUTCROP

The direction of flowing brine (the average or dominant direction of the currents oversaturated with calcium sulphate) should coincide with the dominant orientation of sabre crystal apices. As it was noticed, to find this direction precisely it is

necessary to measure orientation of the individual crystal apices in a statistic way. The methodology used for this work allows to find this direction only in a slightly less precise way. The palaeocurrents surely should pass between limited azimuths of measured azimuth intervals. For simplification the author arbitrarily assumed, as the most probable, that the dominant current was parallel to the bisectrix of the angle between the limited azimuths (i.e. to a bisectrix of azimuth fan). This assumption seems to hold true especially for the narrower azimuth intervals (azimuth spans less than 90°).

The measurements revealed that the azimuth spans varied from 15° to 315° , most commonly ranging from 45° to 125° , with a maximum at 90° (Fig. 5C, bottom). It is interpreted that narrower azimuth intervals reflect more unidirectional flow of brine. Particularly, it seems that the azimuth spans less than about 95° represent strongly unidirectional flow.

The very broad azimuth intervals (especially those with spans over 125°) are more difficult for univocal interpretation. One possibility is that brine currents frequently changed the flow directions, i.e. currents were multidirectional in such localities. The other possibility is that the currents, for some reasons, only weakly influenced the growing crystals. The currents could be very slow, or rare, so that gypsum crystallized mostly in an unmoving brine and crystal apices tend to be directed in diverse horizontal directions (Fig. 2A). Extremely broad azimuth intervals mean that the orientation of crystals is very differentiated and possibly two or more dominating orientations exist (see data from localities 4, 80 in Appendix 1). In such cases more observations and statistic measurements of individual sabre crystals are required for correct interpretation. The broad azimuth intervals are thus less reliable palaeocurrent indicators than the narrow intervals.

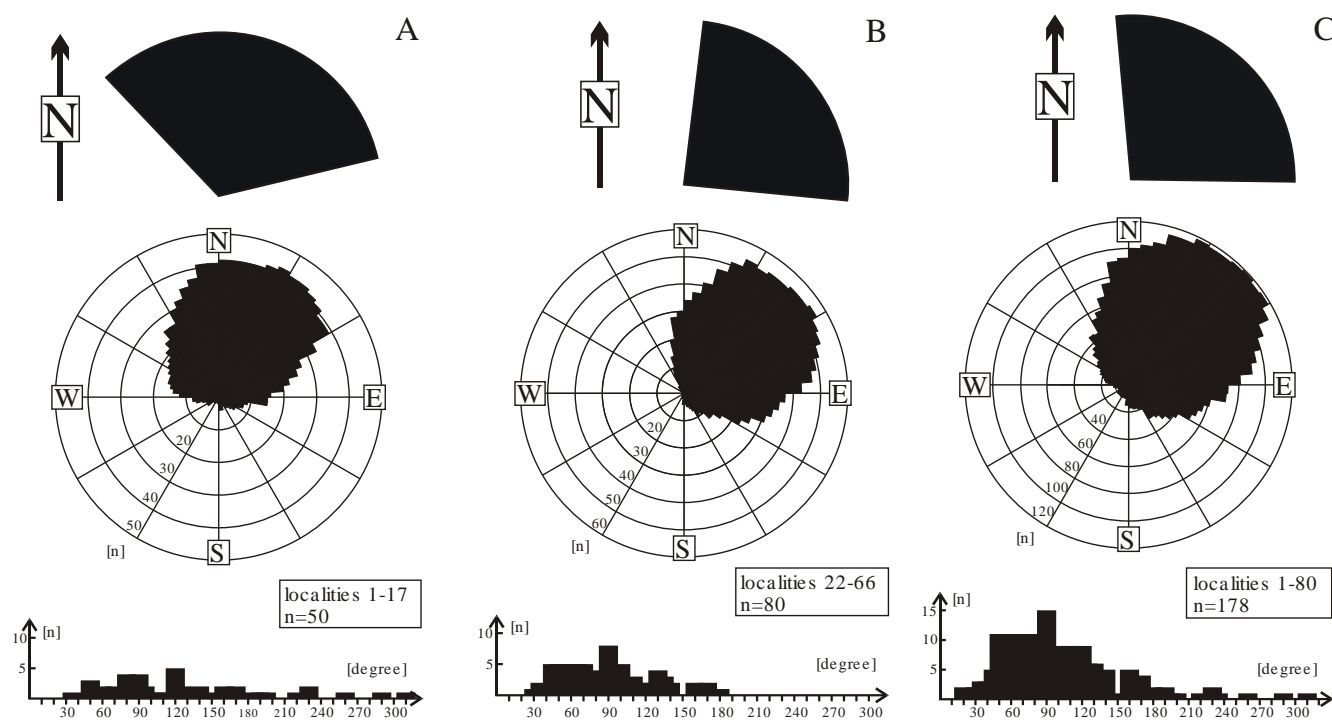


Fig. 5. Statistic characteristics of measured selenite structures

A — for northern area of uniform brine flow; **B** — for southern area of uniform brine flow; **C** — for the whole Nida area; bottom — diagram showing frequency distribution of measured azimuth spans; *n* — number of measured azimuth spans; centre — unconventional circle diagram showing frequency distribution of measured azimuth intervals; *n* — number of measured azimuth intervals; top — simplified mean azimuth fan, limited by two mean vectors; one for all the left and second one for all the right limited azimuths of the measured azimuth intervals

REGIONAL PATTERN OF PALAEOCURRENTS — RULES OF INTERPRETATION

The spatial brine flow pattern is analyzed from distribution of azimuth fans on the map (Figs. 6C–F). Although the palaeocurrent directions are not shown univocally on such a map the possible interpretations are reasonably limited by azimuth spans. The supposed streamlines should be always within the limited pair of azimuths. The broad azimuth fans permit accept more variable directions of palaeoflows which are suitable with adjacent fans.

The other, simplified way of interpretation is to draw the flow directions as vectors which coincide with the bisectrices of azimuth fans. One should, however, remember that such vectors are not precise reflection of dominated orientation of sabre crystal apices such as those found from statistic measurements of individual sabre crystal apices (as in the previous palaeocurrent reconstructions; B bel *et al.*, 1999; Roman, 1999). Because of that this univocal method of interpretation is slightly falsified.

One of the most apparent and important features visible on map of azimuth fans is that on some areas all the adjacent fans are conformably or nearly conformably oriented (Fig. 6C, E). Evidently on these areas the brine flowed very uniformly and continuously in one and the same direction (Fig. 5A, B). The more narrow and more parallel are the fans, the more unidirectional was the brine palaeocurrent in the area. Palaeocurrent di-

rections indicated by such groups of azimuth fans are very reliable. The parallel position of adjacent fans supports the correctness of singular measurements independently made in particular outcrops. The areas with such uniform palaeoflow probably represent the flat bottom without any significant obstacles for the streamlines. Alternatively, such areas can also represent more or less broad inlets where the unidirectional flow was forced by presence of adjacent shoals or islands.

In contrast, closely situated but variably directed or opposite azimuth fans are less reliable and more difficult to apply an univocal interpretation without additional field investigations. Such fans can represent currents flowing in many variable directions for example between complicated network of shoals and islands. On the other hand some fans can represent accidentally oriented sabre crystals, or crystals reoriented by some post-depositional transport; sediment creep, slumps (observed in layer *i*, and sometimes difficult to recognize in pure exposures). In extreme cases some reversely directed fans can be a result of mistakes made during collection or transformation of data.

EVOLUTION OF BRINE PALAEOFLOW

The measurements were also controlled stratigraphically, which permitted a demonstration of the evolution of brine flow directions with time. The azimuth fans or summary azimuth fans for particular layers or groups of layers were transformed

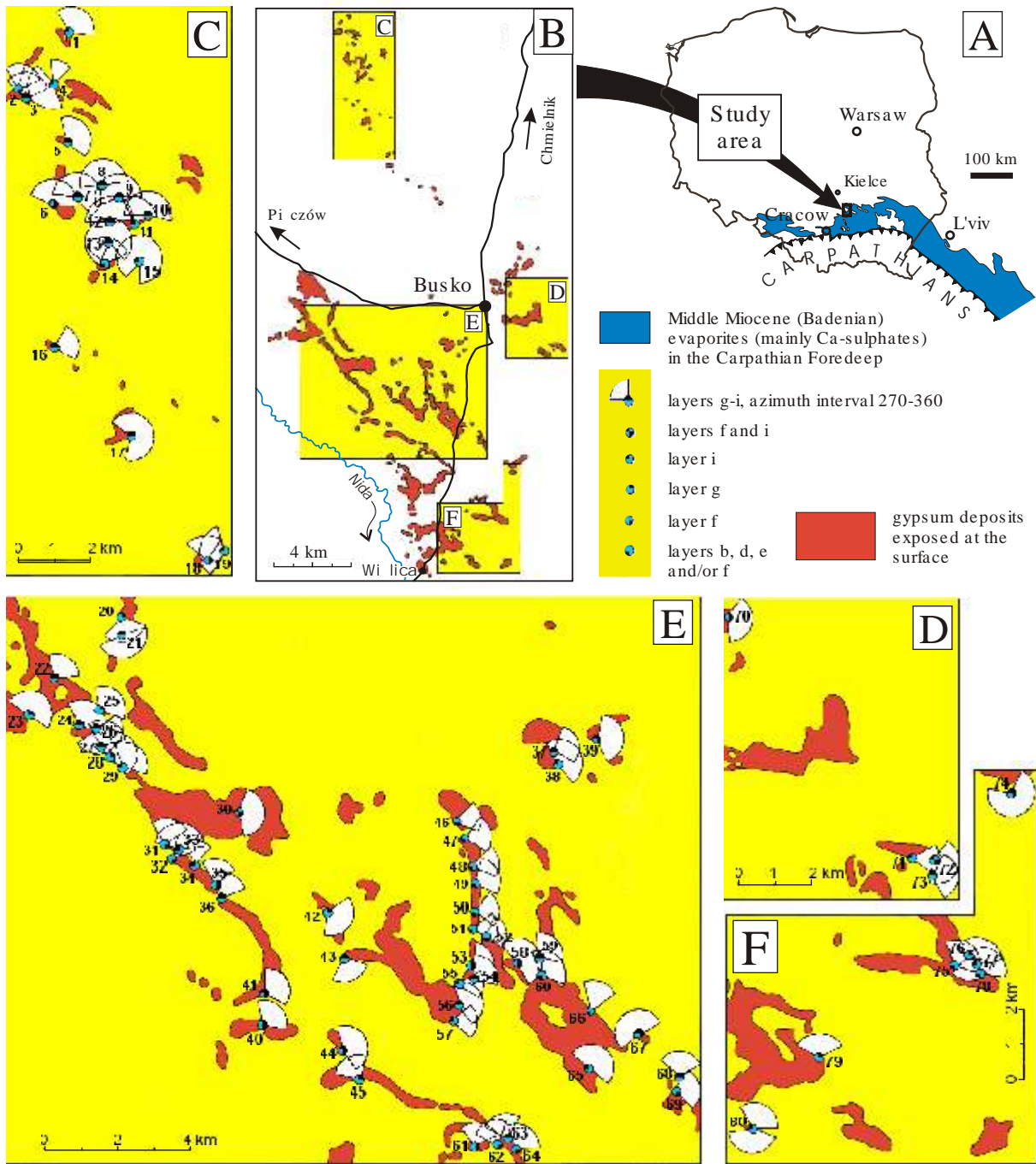


Fig. 6. **A** — Location of the study area of the Middle Miocene (Badenian) evaporites; **B** — Exposures of the Middle Miocene (Badenian) Nida Gypsum deposits (after Senkowicz, 1958; Łyczewska, 1972; Walczowski, 1975; and author's own data); **C–F** — Distribution of measured azimuth fans of oriented selenite crystals in studied localities; complete data set in [Appendix 1](#)

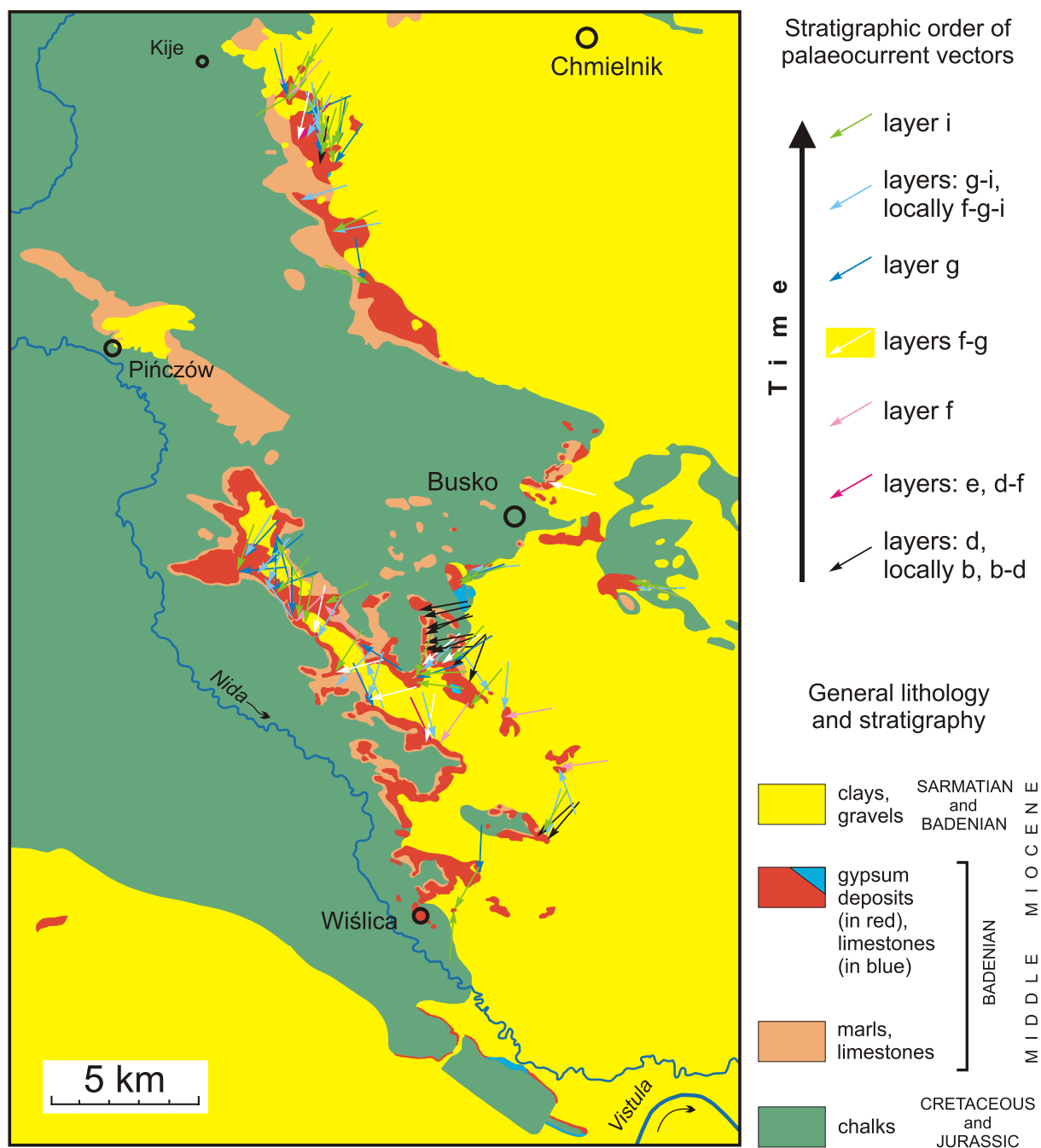


Fig. 7. Changes of brine flow directions during gypsum deposition in the Nida area

Palaeocurrent vectors coincide with bisectrices of azimuth fans (see Appendix 1 for full data set); geological map without Pliocene and Quaternary after Senkowicz 1958; Osmólski, 1972; Łyczewska, 1972, 1975; Walczowski 1975; Wytrwalski, 1976; Jurkiewicz and Wojski, 1979; Rutkowski, 1981; Romanek, 1982; Wojski, 1989; and author's own data

into palaeocurrent vectors (parallel to bisectrices of the azimuth fans; Appendix 1) which, designated by different colors, are shown on the map (Fig. 7). The pattern of colored vectors gives an insight into the changing flow through time. However, any pronounced regularities in the flow changes were not detected. The changes of flow directions in particular localities commonly did not exceed 90° . It seems that the brine flowed all the time in generally the same direction.

RECONSTRUCTION OF PALAEOCURRENTS ON THE NIDA AREA

The 178 azimuth intervals measured in 80 sites on the Nida area were transformed into 80 summary azimuth fans and 80 palaeocurrent vectors and shown on the maps (Figs. 6 and 8). Because the fans represent different time intervals the maps show only a very general picture of brine flow pattern during deposition of broad interval of the section (layers b, d, f, g, i).

The main feature seen on the maps is a dominant direction of brine flow from NE to SW (Figs. 5, 6 and 8). This direction is roughly parallel to the basin outline (Fig. 6A) and fits well to the general brine flow pattern already recognized in the Badenian evaporite basin. As it was mentioned the previous study revealed broad longshore brine stream (or streams) flowing along the northern margin of the basin, from Ukraine to Czech Republic, in the same counterclockwise direction (Bel *et al.*, 1999). This longshore current is well recorded in the study area.

The distribution and orientation of azimuth fans permit to recognition of three uniform brine flows on the Nida area (Figs. 6 and 8). Two such streams inflow onto the study area (one at north at environs of Stawiany, and the second one at east at environs of Busko) and third stream flowed out of the study area (at south-west, between Gacki and Skotniki Dolne). The brine inflowing from the north moved very uniformly between Marynka, Oglódówek and Gartatowice, nearly always predominantly to the south (Fig. 5A). At Chwałowice and Borków this brine turned its flow to the SE and flowed out of the area of recent gypsum exposures. The largest brine stream appears at environs of Busko, strictly between Pczelice, Łągiewniki, Siesławice and Skorocice, where the brine flowed predominantly from east to west. This stream was probably connected with the brine stream between Gacki and Skotniki Dolne where brine predominantly flowed from NE to SW. To the south of this area brine was evidently supplied by inflow from the environs of Siesławice and Skorocice. Thus it seems that one large current flowed across the whole area (Fig. 5B); the brine inflowed from east, from environs of Pczelice, flowed through the area of Siesławice, slightly turning to the left, and between Wola Zagojska and Skotniki Dolne outflowed from the area of gypsum exposures to SW. This evidently indicates that extent of evaporite deposits between Wola Zagojska and Skotniki Dolne is limited by erosion. The evaporite basin continued further towards SW and was fully connected with the evaporite basin of the Miechów Upland (Roman, 1999). The deviations from the uniform brine flow occur at north (at Uników), and in many places at south of the Nida area (at Aleksandrów, Gluzy, Chotel Czerwony and Bilczów). This reflects occurrence of shoals and islands disturbing the brine flows.

CORRECTNESS OF INTERPRETATION

Validity of the interpreted pattern of palaeocurrents can be tested by comparison with other well known palaeocurrent indicators. In the Nida area palaeoflow is also indicated by elongation of microbial domes (Figs. 3 and 4) and were measured at several sites in layer e by Kwiatkowski (1970, fig. 4; 1972, fig. 14). His data drawn on the map (Fig. 8) fit well with the presented reconstruction. At 4 localities situated within the areas of uniform brine flow, the elongation of microbial domes coincides perfectly with palaeocurrents detected from selenite crystal orientations in overlying layers f, g and i (Figs. 6–8). This indicates that during deposition of the lower interval of the sequence (from layer e to i) the direction of brine flow was the same on these areas. Only at 2 localities (Chwałowice and

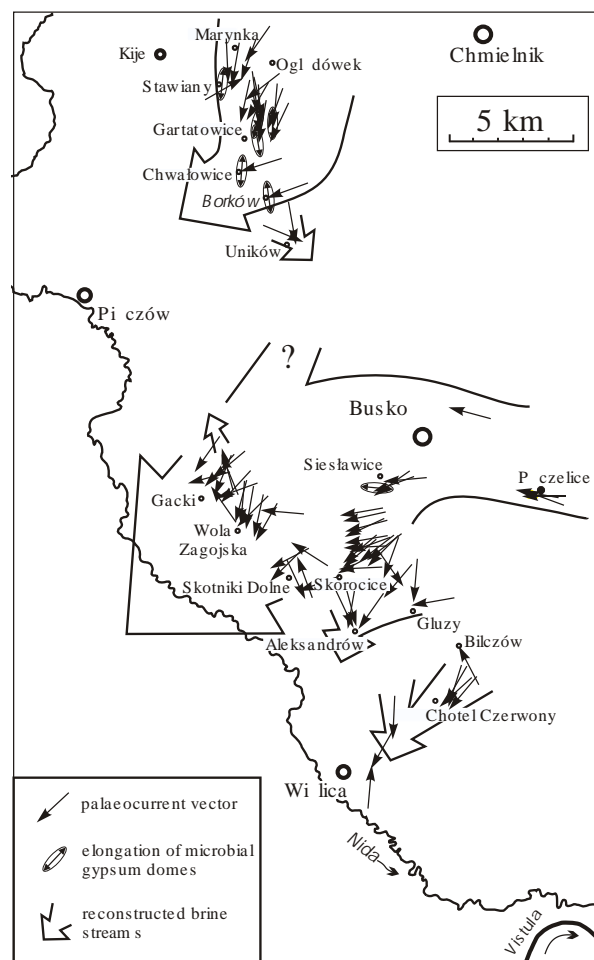


Fig. 8. Simplified interpretation of brine flow pattern on the Nida area

Palaeocurrent vectors coincide with bisectrices of azimuth fans shown in Fig. 6; elongation of gypsum microbial domes after Kwiatkowski (1970, 1972), supplemented at locality Borków (mean of 72 measurements)

Borków) the microbial domes suggest a change of the flow direction during the deposition of the mentioned layers.

FINAL REMARKS

Classic palaeocurrent analysis requires statistic measurements. This requirement is often limited by lack of good exposures and scarcity of palaeocurrent indicators but sometimes also by the short time available for field work. This paper proves that single simplified measurements of selenite crystal orientation made in many adjacent outcrops can bring a good result in palaeocurrent reconstruction in evaporite basin.

The result is successful because of the specific nature of detected palaeocurrents and of the measured features. The studied selenite structures reflect long-termed brine movement, most probably constant longshore circulation as observed in recent lakes and lagoons. Such long-termed flows were probably relatively slow. They were different from strong episodic currents promoted by storms, or catastrophic floods, which produce directional sedimentary structures in the clastic deposits. Strong

storm currents also operated in the basin (Kwiatkowski, 1966, 1972) but they rather tend to destroy or dissolve selenite deposits and had a minor influence on the growth of crystals.

The Badenian evaporite basin, like many other evaporite basins, had a flat bottomed topography and showed only negligible deviations. Because of the evolving basin form the brine flowed over large areas constantly in one direction over relatively long period of time — enough for crystallization a thick selenite strata (up to 12 m). The flowing brine influenced the growth of gypsum crystals practically on every place of the bot-

tom. As a result the oriented selenite crystals, unlike the directional structures of clastic deposits, are so apparent and recorded in every outcrop.

Acknowledgments. The author thanks Stanisław Matysiak for help in statistic calculations and Grzegorz Czapowski, Marek Narkiewicz and B. Charlotte Schreiber for their careful reviews of that paper and critical comments which improved its final version. The research was partly sponsored by the KBN grant 6 P04D 038 09 given to the author.

REFERENCES

- B BEL M. (1986) — Growth of crystals and sedimentary structures of the sabre-like gypsum (Miocene, southern Poland). *Prz. Geol.*, **34** (4): 204–208.
- B BEL M. (1996) — Wykształcenie facjalne, stratygrafia oraz sedimentacja bade skich gipsów Poniidzia. In: *Analiza basenów sedimentacyjnych a nowoczesna sedimentologia* (ed. P. H. Karnkowski): B1–B26. Materiały Konferencyjne V Krajowego Spotkania Sedymetologów. Warszawa.
- B BEL M. (1999a) — Facies and depositional environments of the Nida Gypsum deposits (Middle Miocene, Carpathian Foredeep, southern Poland). *Geol. Quart.*, **43** (4): 405–428.
- B BEL M. (1999b) — History of sedimentation of the Nida Gypsum deposits (Middle Miocene, southern Poland). *Geol. Quart.*, **43** (4): 429–447.
- B BEL M. (2000) — Anisotropic development of equivalent gypsum crystal faces promoted by chiral organic compounds. In: *Mineralogy and Life: Biomineral Homologies* (eds. N. P. Yushkin, V. P. Lutoev, M. F. Samotolkova., M. V. Gavriluk and G. V. Ponomareva), 3th Intern. Seminar Mineralogy and Life, Abstracts: 132–133. Syktyvkar.
- B BEL M., BOGUCKIY A., VIZNA S. and YATSYSHYN A. (1999) — Reconstruction of brine paleocurrents in the Middle Miocene evaporitic basin of the Carpathian Foredeep. Intern. Symp. "Evaporites and carbonate-evaporate transitions". *Biul. Pa stw. Inst. Geol.*, **387**: 12–13.
- BOBROWSKI W. (1963) — Gypsum in the eastern bank of the Nida river valley (in Polish with English summary). *Biul. Inst. Geol.* (without number): 1–29.
- CODY A. M. and CODY R. D. (1991) — Chiral habit modifications of gypsum from epitaxial-like adsorption of stereospecific growth inhibitors. *J. Crystal Growth*, **113**: 508–519.
- CODY R. D. and CODY A. M. (1991) — Gypsum nucleation and crystal morphology in analog saline terrestrial environments. *J. Sed. Petrol.*, **58** (2): 247–255.
- DRONKERT H. (1977) — The evaporites of the Sorbas basin. *Inst. Invest. Geol. Diput. Prov. Univ. Barcelona*, **32**: 55–76.
- DRONKERT H. (1978) — Late Miocene evaporites in the Sorbas Basin and adjoining areas. *Mem. Soc. Geol. Italiana*, **16**: 341–361.
- DRONKERT H. (1985) — Evaporite models and sedimentology of Messinian and Recent evaporites. *GUA Papers of Geology, Ser. 1*, **24**.
- FIJAŁKOWSKA E. and FIJAŁKOWSKI J. (1968) — Occurrence of gypsum in the wi tokrzyskie Mountains (in Polish with English summary). *Rocznik Muzeum wi tokrzyskiego*, **7**: 303–336.
- FLIS J. (1954) — Gypsum karst of the Nida Trough (in Polish with English summary). *Pr. Geogr., Inst. Geogr. PAN*, **1**.
- HILGERS C. and URAI J. L. (2002) — Experimental study of syntaxial vein growth during lateral fluid flow in transmitted light: first results. *J. Struct. Geol.*, **24** (6–7): 1029–1043.
- JURKIEWICZ H. and WOI SKI J. (1979) — Mapa geologiczna Polski, 1: 200000. Arkusz Tarnów (B). *Wyd. Geol. Warszawa*.
- KASPRZYK A. (1993a) — Lithofacies and sedimentation of the Badenian (Middle Miocene) gypsum in northern part of the Carpathian Foredeep, southern Poland. *Ann. Soc. Géol. Pol.*, **63** (1–3): 33–84.
- KASPRZYK A. (1993b) — Gypsum facies in the Badenian (middle Miocene) of southern Poland. *Can. J. Earth Sc.*, **30** (9): 1799–1814.
- KASPRZYK A. (1994) — Distribution of strontium in the Badenian (Middle Miocene) gypsum deposits of the Nida area, southern Poland. *Geol. Quart.*, **38** (3): 497–512.
- KASPRZYK A. (1995) — Correlation of sulphate deposits of the Carpathian Foredeep at the boundary of Poland and Ukraine. *Geol. Quart.*, **39** (1): 95–108.
- KASPRZYK A., PERYT T. M., TURCHINOV I. I. and JASIONOWSKI M. (1999) — Badenian gypsum in the Poniidzie area, the northern Carpathian Foredeep, Poland. Intern. Conference "Carpathian Foredeep Basin — its evolution and mineral resources", Excursion 5: 1–21. Kraków.
- KUBICA B. (1992) — Lithofacial development of the Badenian chemical sediments in the northern part of the Carpathian Foredeep (in Polish with English summary). *Prace Pa stw. Inst. Geol.*, **133**.
- KWIATKOWSKI S. (1966) — Cross-bedding in Miocene Gypsum of Nida Valley. *Bull. Acad. Pol. Sc., Sér. Sc. Géol. Géogr.*, **16** (3): 155–156.
- KWIATKOWSKI S. (1970) — Origin of alabasters, intraformational breccias, folds and stromatolites in Miocene gypsum of Southern Poland. *Bull. Acad. Pol. Sc., Sér. Sc. Géol. Géogr.*, **18** (1): 37–42.
- KWIATKOWSKI S. (1972) — Sedimentation of gypsum in the Miocene of southern Poland (in Polish with English summary). *Pr. Muz. Ziemi*, **19**: 3–94.
- KWIATKOWSKI S. (1974) — Miocene gypsum deposits in southern Poland (in Polish with English summary). *Biul. Inst. Geol.*, **280**: 299–344.
- ŁYCZEWSKA J. (1972) — Szczegółowa mapa geologiczna Polski, 1: 50000. Arkusz Busko Zdrój. *Wyd. Geol. Warszawa*.
- ŁYCZEWSKA J. (1975) — An outline of the geological structure of the Wójcza-Pi czów Range (in Polish with English summary). *Biul. Inst. Geol.*, **283**: 151–188.
- NEWHOUSE W. H. (1941) — The direction of flow of mineralizing solutions. *Econ. Geol.*, **36** (6): 612–629.
- NIEMCZYK J. (1997) — Miocene slumps in the gypsum series of Siesławice near Busko Zdrój and geology of the region (Central Poland) (in Polish only). *Prz. Geol.*, **45** (8): 811–815.
- OSMÓLSKI T. (1972) — The influence of the geological structure of the marginal parts of the Działoszyce trough on the metasomatism of gypsum (in Polish with English summary). *Biul. Inst. Geol.*, **260**: 65–188.
- ORTÍ CABO F., PUEYO MUR J. J., GEISLER-CUSSEY D. and DULAU N. (1984) — Evaporitic sedimentation in the coastal salinas of Santa Pola (Alicante, Spain). *Rev. Inst. Invest. Geol.*, **38–39**: 169–220.
- PAWLIKOWSKI M. (1982) — Mineralogical and petrographical study of alteration products of the Miocene gypsum rocks in the Wydrza sulphur deposit (in Polish with English summary). *Pr. Miner., Komis. Nauk Miner. PAN, Kraków*, **72**.
- PERYT T. M. (1996) — Sedimentology of Badenian (middle Miocene) gypsum in eastern Galicia, Podolia and Bukovina (West Ukraine). *Sedimentology*, **43** (3): 571–588.

- PERYT T. M. (2001) — Gypsum facies transitions in basin-marginal evaporites: middle Miocene (Badenian) of west Ukraine. *Sedimentology*, **48** (5): 1103–1119.
- PETRICHENKO O. I., PERYT T. M. and POBEREGSKY A. A. (1997) — Peculiarities of gypsum sedimentation in the Middle Miocene Badenian evaporite basin of Carpathian Foredeep. *Slovak Geol. Mag.*, **3** (2): 91–104.
- PRIETO M., PANIAGUA A. and MARCOS C. (1996) — Formation of primary fluid inclusions under influence of the hydrodynamic environment. *European J. Miner.*, **8** (5): 987–996.
- RODRIGUEZ-NAVARRO A. and GARCIA-RUIZ J. M. (2000) — Model of textural development of layered crystal aggregates. *European J. Miner.*, **12** (3): 609–614.
- ROMAN A. (1999) — Brine paleocurrents reconstructed from orientation of the gypsum crystals on the Miechów Upland, Southern Poland. Intern. Symp. “Evaporates and carbonate-evaporate transitions”. Abstracts. Lviv. Biul. Pa. stw. Inst. Geol., **387**: 60–62.
- ROMANEK A. (1982) — Szczegółowa mapa geologiczna Polski, 1: 50000. Arkusz Chmienik. Wyd. Geol. Warszawa.
- RUTKOWSKI J. (1981) — The tectonics of miocene sediments of the western part of the Połaniec graben (Carpathian Foredeep, southern Poland) (in Polish with English summary). *Rocznik Pol. Tow. Geol.*, **51** (1–2): 117–131.
- SENKOWICZ E. (1958) — Szczegółowa mapa geologiczna Polski, 1: 50000. Arkusz Pi czów. Wyd. Geol. Warszawa.
- WALA A. (1961) — Litológia mioce skiej serii ewaporatów w okolicy Pi czowa. Sprawozdania z Pos. Komis. Nauk. PAN, Kraków, **1/6**: 275–280.
- WALA A. (1963) — Korelacja litostratygraficzna serii gipsowej obszaru nadnidzia skiego. Sprawozdania z Pos. Komis. Nauk. PAN, Kraków, (1962), **7–12**: 530–532.
- WALA A. (1980) — Litostratygrafia gipsów nízdzia skich (fm). In: Gipsy niecki nízdzia skiej i ich znaczenie surowcowe: 5–10. Symp. Nauk. Kraków.
- WALCZOWSKI A. (1975) — Szczegółowa mapa geologiczna Polski, 1: 50000. Arkusz Stopnica. Wyd. Geol. Warszawa.
- WOI SKI J. (1989) — Szczegółowa mapa geologiczna Polski, 1: 50000. Arkusz Działoszyce. Wyd. Geol. Warszawa.
- WYTRWALSKI K. (1976) — Mapa geologiczna obszaru Busko-Wi lica 1:25000. In: Przebieg i prognozowanie procesów egzogenicznych na obszarze plateau gipsowego Busko-Wi lica w aspekcie ochrony rodowiska geologicznego. Unpublished MSc Thesis. Univ. Warsaw.
- ZEJSZNER L. (1861) — O mijoceniczych gipsach i marglach w południowo-zachodnich stronach Królestwa Polskiego. *Biblioteka Warszawska*, **4** (10): 230–245; (11): 472–487; (12): 715–733.

APPENDIX 1

Localities with measured orientation of selenite crystals

Description of outcrops are given in Zejszner, 1861; Flis, 1954; Bobrowski, 1963; Fijałkowska and Fijałkowski, 1968; Kwiatkowski, 1972, 1974; Kasprzyk *et al.*, 1999, and in many other papers (see references in Kwiatkowski, 1972, 1974; B el, 1999a). The best sections exposed at localities 2, 9–13, 15–17, 22–28, 37–38, 43, 53–57, 68, 74, 78 are documented by Wala, 1961, 1963; Kasprzyk, 1994; B el, 1996, 1999b

No.	Description of locality	Measurements (in degrees)	Sum of all measurements (in degrees)	Bisectrix of sum of all measurements (in degrees)	Bisectrices of sum of measurements for particular layers (in degrees)
1	Marynka-Ogl dówek, abandoned quarries	20–100, 10–100, 340–100, 330–100 (layer I)	330–100	35	–
2	Stawiany, abandoned quarry at NE edge of village, N of road to Samostrzałów	320–35 (layer f)	320–35	357.5	–
3	Stawiany, water-filled quarries on both sides of road to Samostrzałów	25–60 (layer f), 320–10 (layer g), 340–30 (layers g–i), 350–60 (layer i)	320–60	10	f 42.5 g 345 i 25
4	Stawiany-Ogl dówek; abandoned quarries at bottom of valley nearby railroad and stream	160–320, 350–50 (layer i)	160–320 350–50	240, 20	–
5	Stawiany, karst area in valley E of village, between hills and stream	30–120, 15–75, 35–115 (layer g), 350–75, 350–40, 345–70 (layer i)	345–120	52.5	g 67.5 i 30
6	Gartatowice-Stawiany, westernmost abandoned quarries near country road N of Stawiany-Bogoria railroad	0–80 (layers d–f), 345–90, 315–40, locally 295 (layers f, g)	295–90	12.5	d–f 40 f, g 12.5
7	Gartatowice-Stawiany, abandoned quarries N of Stawiany-Bogoria railroad	285–45, 275–145 (layers g–i)	275–145	30	–
8	Gartatowice-Stawiany, easternmost abandoned quarries, N of junction of railroads	260–85 (layers g–i)	260–85	352.5	–

Appendix 1 continued

1	2	3	4	5	6
9	Gartatowice, two northernmost abandoned quarries, S of Stawiany-Bogoria railroad, 120–260 m E of railroad to quarries, SE quarry with layers g-i and SW quarry with layer i	255–20, 255–60 (layers g-i), 250–85 (layer i)	250–85	347.5	g-i 337.5 i 347.5
10	Gartatowice-Zajezerze, northeasternmost abandoned quarries	335–65, 305–65, 340–50 (layer g), 270–30, 270–60, 270–100 (layer i)	270–100	5	g 10 i 5
11	Gartatowice-Zajezerze, northern abandoned quarries	335–65 (layer i)	335–65	20	–
12	Gartatowice, abandoned quarries within turning of railroad, N part of nature reserve	270–80 (layers g-i), 320–60, 320–85, 275–85 (layer i)	270–85	357.5	g-i 355 i 0
13	Gartatowice, water-filled quarries at nature reserve, N of road to S dziejowice	330–65, 310–70, 295–75, locally 205–135 (layer g), 330–65 (layer i), 300–100 (layers g-i)	205–135	350	g 350 i 17.5
14	Gartatowice, water-filled quarry 250 m S of road to S dziejowice	315–65 (layers b-d)	315–65	347.5	–
15	Gartatowice-Zajezerze, abandoned quarries S of road to S dziejowice	230–130, locally 230–180 (layer g), 280–60 (layer i)	230–180	35	g 35 i 350
16	Chwałowice, abandoned quarry W of road to Gartatowice	40–105 (layers g-i)	72.5	–	–
17	Borków quarry	330–190 (layers g-i) 310–180 (layer i)	310–190	70	g-i 80 i 65
18	Uników, S part of abandoned quarries between road and stream	310–30; commonly at 348 and 18 (layer g)	310–30	350	–
19	Uników-Skały, abandoned quarries near forest	260–325; commonly at 293 (layer i)	260–325	292.5	–
20	Marz cin, karst sink holes near country road	110–220 (layer g)	110–220	165	–
21	Marz cin, small hills near country road	140–245 (layer g) 115–230, 70–230 (layer i)	70–245	157.5	g 180 i 150
22	Gacki quarry, 300 m NW of wayside cross near road to Bogucice	345–80 (layers g-i), 0–85 (layer g)	345–85	35	g 42.5 g-i 32.5
23	Gacki, hills near entrance to large abandoned quarry	20–190 (layer g), 310–90 (layer i)	310–190	75	g 85 i 20
24	Leszcze, west slope of hill in W part of quarry, E of road Gacki-Bogucice	335–110 (layers g-i)	335–110	42.5	–
25	Sołectwo, north escarpment of ravine NW of Leszcze quarry	350–110 (layer g)	350–110	50	–
26	Leszcze, west-central part of quarry	55–235 (layers g-i)	55–235	145	–
27	Leszcze, hill W of entrance to quarry	330–75 (layers g-i)	330–75	225	–
28	Leszcze, hill E of entrance to quarry	5–135 (layer g)	5–135	70	–
29	Wola Zagojska-Górna, 2nd hill 250 m E of entrance to Leszcze quarry	340–105 (layer i)	340–105	42.5	–
30	Winiary, two abandoned quarries N of village, layer f at N, layer i 50 m at S	100–170 (layer f), 20–110 (layer i)	20–170	95	f 135 i 65
31	Wola Zagojska-Górna, west slope of hill, 200 m W of Winiarski stream karst spring	345–45, 330–20, 350–50 (layer f), 330–60, 350–35 (layer g)	330–60	0	f 355 g 0
32	Wola Zagojska-Górna, Winiarski stream karst spring	340–25, 335–40, 285–85, 15–65, 15–50 (layer i)	285–85	5	–

Appendix 1 continued

1	2	3	4	5	6
33	Wola Zagojska-Górna, hill 150 m SW of Winiarski stream karst spring	25–75, 15–70 (layer f)	15–75	45	–
34	Winiary, near country road passing hill S of village	340–40 (layer i)	340–40	10	–
35	Winiary-Zago, road cut through escarpment of Nida River valley, west hill	345–30, 5–35, 345–40, 345–55, 330–55, commonly 345–30 (layers f, g)	330–55	12.5	–
36	Winiary-Zago, road cut through escarpment of Nida River valley, east hill	350–70 (layers g–i)	350–70	30	–
37	Siesławice, abandoned northern quarry	20–85, 35–95, 40–120 (layer g), 25–120 (layer i)	20–120	70	g 70 i 72.5
38	Siesławice; abandoned southern quarry W of road to Chotelek	15–85, 355–135, 330–140 (layer i)	330–140	55	–
39	Siesławice, small hill E of road	15–115, 25–155 (layers f, g or i)	15–155	85	–
40	Skotniki Dolne, near spring NW of village	350–100, 350–100, 350–100 (layers g–i)	350–100	45	–
41	Skotniki Górne nature reserve, railroad cut	30–120 (layers f, g), 5–60 (layer i)	5–120	62.5	f, g 75 i 32.5
42	Skotniki Górne-Winiary, east slope of small valley	55–190 (layer g)	55–190	122.5	–
43	Skotniki Górne-Waty, hill with karst cave	145–210, 110–160 (layers g–i)	110–210	160	–
44	Skotniki Dolne; three outcrops within distance of 100 m, between Skotnicki stream and main road to Skorocice	350–150 (layers f, g), 0–35 (layers g–i), 30–150 (layers f, g–i)	350–150	70	f, g 70 g–i 17.5
45	Skotniki Dolne, outcrop near road in E part of village	290–20, 280–20 (layer g)	290–20	335	–
46	Chotelek Zielony, southern escarpment of hill 75 m W of road	45–115 (layer b or f)	45–115	80	–
47	Chotelek Zielony, hill SE of road	35–120 (layer d)	35–120	77.5	–
48	Chotelek Zielony-Skorocice, two outcrops: cut of country road and small hill 100 m to S (7th one N of spring at Skorocice nature reserve)	40–110, 40–90 (layer d)	40–110	75	–
49	Chotelek Zielony-Skorocice, west slope of small hill near country road (6th one N of spring at Skorocice nature reserve)	15–105, 25–115 (layer d)	15–115	65	–
50	Chotelek Zielony-Skorocice, top of small hill (5th one N of spring at Skorocice nature reserve) near country road	35–125, 50–125 (layer d)	35–125	80	–
51	Chotelek Zielony-Skorocice, south part of small hill (4th one N of spring at Skorocice nature reserve)	75–120, 50–125 (layer d)	50–125	87.5	–
52	Chotelek Zielony-Skorocice, west escarpment of hill, E of country road	20–120 (layer b or f)	20–120	70	–
53	Skorocice, hill W of pond in N part of nature reserve	10–90 (layers f, g)	10–90	50	–
54	Skorocice nature reserve, Kazalnica hill	0–100, 10–75 (layers g–i)	0–100	50	–
55	Skorocice nature reserve, environs of Wielka hill	55–120 (layer i)	55–120	87.5	–
56	Skorocice nature reserve, environs of Biała hill	10–135 (layer g), 350–50 (layer i)	350–135	62.5	g 72.5 i 20
57	Skorocice nature reserve, S entrance to karst valley	45–150 (layer i)	45–150	97.5	–
58	Skorocice-Łatanice, south slope of hill NE of nature reserve, near gypsum dome	20–150, 50–150, locally 315–90 (layers f, g)	315–150	52.5	–
59	Skorocice-Łatanice, escarpments on N slope of hill SW of stream	15–110 (layer g), 355–90 (layer i), 0–80 (layers g–i)	355–110	52.5	g 57.5 i 42.5

Appendix 1 continued

1	2	3	3	4	5
60	Skorocice-Łatanice, karst area among meadows in valley	340–110, 0–90 (layer d)	340–110	45	–
61	Aleksandrów, outcrop near road	320–60 (layers f, g)	320–60	10	–
62	Aleksandrów, karst spring near road	300–20, 290–20 (layer e)	290–20	335	–
63	Aleksandrów, gypsum dome in karst valley	300–20, 320–30 (layers g–i)	300–30	345	–
64	Aleksandrów, east entrance to karst valley	345–85, 350–50 (layer f)	345–85	35	–
65	Łatanice, near country well in karst area W of road Busko-Wi lica	310–130 (layer i)	310–130	40	–
66	Łatanice, abandoned quarry W of village	50–350 (layers b–d)	350–50	20	–
67	Łatanice, hill E of village S of road to Hołudza	230–60 (layers f, g–i)	230–60	325	–
68	Hołudza, escarpment at E slope of hill	310–60 (layers g–i)	310–60	5	–
69	Hołudza-Gluzy, small outcrop among meadows near country road	25–135 (layer f)	25–135	80	–
70	Łagiewniki, hill E of spring	45–150, 40–170, commonly 100 (layers f, g)	40–170	105	–
71	Owczary, west slope of small hills S of road to P czelice	70–130 (layer i)	70–130	100	–
72	Owczary-P czelice, north slopes of small hills S of road	60–160 (layer f), 60–90, 60–150, 30–150, 60–80, 100–190, 90–140 (layer i)	30–190	110	f 110 i 110
73	Owczary-P czelice, easternmost small rocky hills W of hill 245.0	30–100, 80–150, at upper part 60–120 (layers g–i)	30–150	90	–
74	Bilczów, two small hills: at SE side of pond (layer f) and 100 m SW at house courtyard N of road (layers f, g–i)	25–140 (layer f), 80–280 (layers f, g–i)	25–280	152.5	f 82.5 f, g–i 160
75	Chotel Czerwony, W part of Góry Wschodnie nature reserve	340–105 (layer d)	340–105	47.5	–
76	Chotel Czerwony-Zagórze, abandoned quarries	320–100 (layer i)	320–100	30	–
77	Chotel Czerwony-Zagórze, abandoned quarries	315–80 (layers g–i)	315–80	17.5	–
78	Chotel Czerwony-Zagórze, easternmost abandoned quarries	340–100 (layer d)	340–100	40	–
79	Gorysławice, small outcrop SE of hill 185.6	300–65 (layer g)	300–65	2.5	–
80	Psia Górka	50–70, 0–70, 50–90, locally 315, 330–25, 320–70, 160–200, 110–190, 190–240, 210–260, 45–85 (layer i)	330–90, 110–260	30, 185	–